

# Myosin light chain kinase binding to a unique site on F-actin revealed by three-dimensional image reconstruction

Victoria Hatch,<sup>1</sup> Gang Zhi,<sup>2</sup> Lula Smith,<sup>2</sup> James T. Stull,<sup>2</sup> Roger Craig,<sup>3</sup> and William Lehman<sup>1</sup>

<sup>1</sup>Department of Physiology and Biophysics, Boston University School of Medicine, Boston, MA

<sup>2</sup>Department of Physiology, University of Texas Southwestern Medical Center at Dallas, Dallas, TX

<sup>3</sup>Department of Cell Biology, University of Massachusetts Medical School, Worcester, MA

**C**a<sup>2+</sup>-calmodulin-dependent phosphorylation of myosin regulatory light chains by the catalytic COOH-terminal half of myosin light chain kinase (MLCK) activates myosin II in smooth and nonmuscle cells. In addition, MLCK binds to thin filaments *in situ* and F-actin *in vitro* via a specific repeat motif in its NH<sub>2</sub> terminus at a stoichiometry of one MLCK per three actin monomers. We have investigated the structural basis of MLCK-actin interactions by negative staining and helical reconstruction. F-actin was decorated with a peptide containing the NH<sub>2</sub>-terminal 147 residues of MLCK (MLCK-147) that binds to F-actin with high affinity. MLCK-147 caused formation of

F-actin rafts, and single filaments within rafts were used for structural analysis. Three-dimensional reconstructions showed MLCK density on the extreme periphery of subdomain-1 of each actin monomer forming a bridge to the periphery of subdomain-4 of the azimuthally adjacent actin. Fitting the reconstruction to the atomic model of F-actin revealed interaction of MLCK-147 close to the COOH terminus of the first actin and near residues 228–232 of the second. This unique location enables MLCK to bind to actin without interfering with the binding of any other key actin-binding proteins, including myosin, tropomyosin, caldesmon, and calponin.

## Introduction

Signal transduction pathways, linking extracellular stimuli to intracellular processes, are essential for regulation of all cells. Their effective operation requires complex spatial and temporal organization that couples the component steps together. Phosphorylation–dephosphorylation pathways, for example, represent major cell control mechanisms, and generally the effector kinases and phosphatases and their protein targets are discretely compartmentalized in cells (Perry, 1983; Cohen, 2000). Myosin II activity, for example in smooth muscle and nonmuscle cells, is regulated by phosphorylation, and the kinase responsible is anchored on actin filaments.

Myosin regulatory light chains are phosphorylated by Ca<sup>2+</sup>-calmodulin-dependent myosin light chain kinase

(MLCK)\* and dephosphorylated by a distinct form of phosphatase type 1 (for reviews see Kamm and Stull, 1985, 2001; Sellers and Adelstein, 1986; Erdödi et al., 1996; Somlyo and Somlyo, 2000). There is no troponin in smooth muscle, and here, as in nonmuscle cells, Ca<sup>2+</sup> binds to its target protein, calmodulin, as cytoplasmic Ca<sup>2+</sup> concentration increases after cell stimulation. The Ca<sup>2+</sup>-calmodulin complex then binds to MLCK, leading to its activation, light chain phosphorylation, increased actin-activated myosin ATPase activity, cross-bridge cycling on thin filaments, and contraction. Both MLCK and phosphatase are modulated by phosphorylation and dephosphorylation, reactions mediated by signaling networks (Stull et al., 1996, 1997; Somlyo and Somlyo, 2000; MacDonald et al., 2001).

There are two genes that express a skeletal muscle specific MLCK and a smooth muscle MLCK, respectively. The smooth muscle MLCK is ubiquitously expressed (Herring et al., 2000) and consists of short and long isoforms due to

Address correspondence to William Lehman, Department of Physiology and Biophysics, Boston University School of Medicine, 715 Albany St., Boston, MA 02118-2526. Tel.: (617) 638-4397. Fax: (617) 638-4273. E-mail: wlehman@bu.edu

L. Smith's current address is Department of Biological Chemistry, Alabama State University, Montgomery, AL 36101.

Key words: actin; electron microscopy; myosin; myosin light chain kinase; phosphorylation

\*Abbreviations used in this paper: 3-D, three-dimensional; MLCK, myosin light chain kinase; MLCK-147; peptide containing the NH<sub>2</sub>-terminal 147 residues of MLCK.

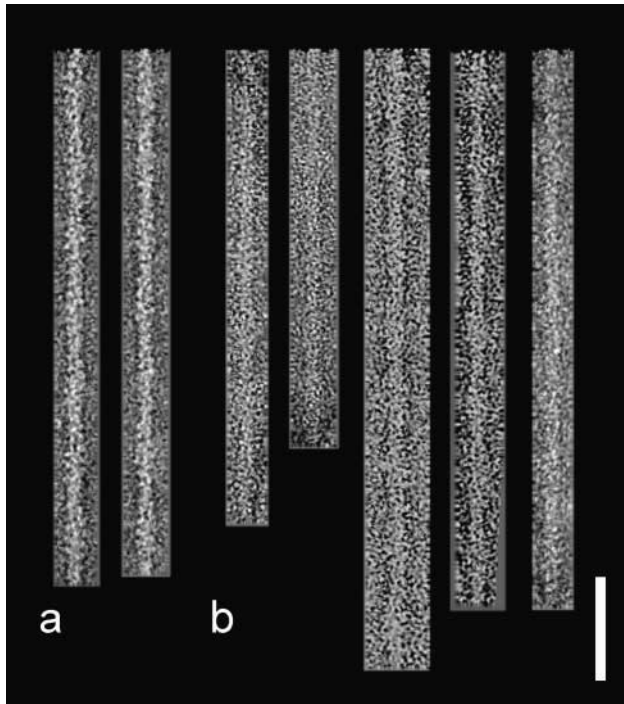


**Figure 1. Electron micrographs of negatively stained filaments.** (a) Rabbit skeletal muscle F-actin alone (two examples). (b) Skeletal muscle F-actin-MLCK-147 (five examples). Note the increased diameter of the decorated F-actin. Bar, 50 nm.

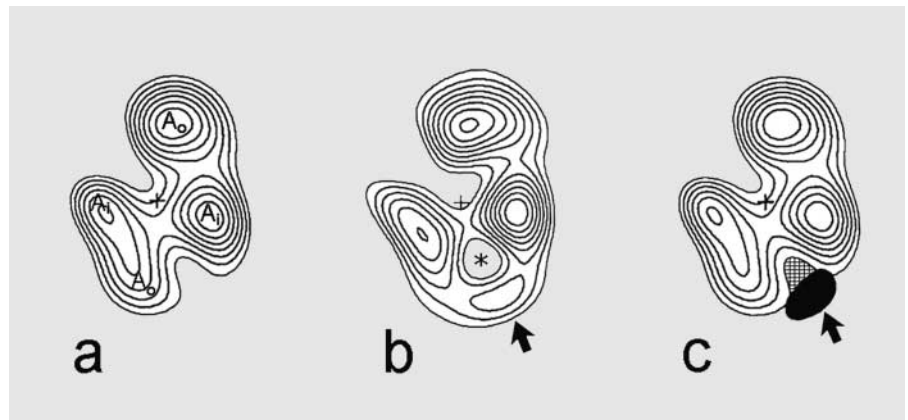
multiple promoters in the gene (Kamm and Stull, 2001). Short MLCK is present in smooth muscle cells at  $\sim 4 \mu\text{M}$  (Hartshorne, 1987; Tansey et al., 1994) in an approximate molar ratio to myosin of 1:10 and to actin in filaments of 1:100. The short MLCK isoform found in smooth muscle and some nonmuscle cells possesses an  $\text{NH}_2$ -terminal actin-binding extension (Kanoh et al., 1993; Gallagher and Stull, 1997; Ye et al., 1997), not present in skeletal muscle MLCK (Nunnally and Stull, 1984; Lin et al., 1997), that localizes the kinase to thin filaments, restricting its cellular mobility

(Guerriero et al., 1981; Dabrowska et al., 1982; Sellers and Pato, 1984). The long MLCK is the same as the short MLCK with additional actin-binding motifs and structural modules at the  $\text{NH}_2$  terminus. The long MLCK has a greater affinity for F-actin and is found primarily in non-muscle cells (Kamm and Stull, 2001), where myosin II-based motility is also regulated by light chain phosphorylation. The resulting compartmentalization of MLCK may be involved in defining contractile regions in both smooth muscle and nonmuscle cells.

The  $\text{NH}_2$ -terminal extensions contain a novel high-affinity actin-binding sequence, DFRXXL, which repeats three times in short MLCK, leading to binding saturation of one MLCK to three actin monomers along F-actin in vitro (Smith et al., 1999; Smith and Stull, 2000). Mutating the binding motifs significantly decreases association of MLCK with myofilaments in vitro and with actin-containing filaments in intact smooth muscle cells (Smith et al., 1999). The full-length short kinase is an elongated molecule, and intervening PEVK, Ig-like, and fibronectin-like repeats between  $\text{NH}_2$ -terminal and more  $\text{COOH}$ -terminal catalytic domains are thought to provide sufficient extension for the catalytic core to reach thick filaments abutting thin filaments (Stull et al., 1996; Lin et al., 1999; Smith and Stull, 2000), thus allowing effective light chain phosphorylation of cross-bridges. A  $\text{COOH}$ -terminal low-affinity myosin-binding fragment in MLCK (Sellers and Pato, 1984) may direct the kinase towards myosin filaments, increasing the probability of myosin phosphorylation during activity, whereas the  $\text{NH}_2$  terminus binds with sufficient high affinity to anchor the kinase to actin filaments. Additionally, since MLCK apparently is not dissociated from thin filaments by  $\text{Ca}^{2+}$  or  $\text{Ca}^{2+}$ -calmodulin (Lin et al., 1999), the enzyme will localize close to thin and thick filaments both at the onset and during contractile activity.

Actin, the core of the thin filament, serves as a molecular track for the myosin cross-bridge motor. Tropomyosin, also present on thin filaments, ensures that on-off switching of myosin ATPase and consequently contractility occurs coop-

**Figure 2. Transverse sections (z-sections) of 3-D reconstructions.** (a) F-actin control. Because adjacent actin monomers are staggered by  $\sim 1/2 \times 55 \text{ \AA}$ , sectioning the reconstruction through the widest part of one actin (monomer on the right) results in sectioning through a narrower part of the adjacent one (on the left); outer and inner domains are marked  $A_o$  and  $A_i$  on each. (b) F-actin-MLCK-147; note the extra density (arrow) due to MLCK on the extreme periphery of the map bridging inner and outer domains of the two actin monomers sectioned. (c) Maps in a and b were compared, and the difference between the two (filled black region) was superimposed on a copy of the F-actin map. The difference densities, attributable to the bound MLCK, were statistically significant at  $>99.95\%$  confidence levels. This analysis also showed that the protein-free pore between the MLCK density and F-actin (\* in b; cross-hatching in c) was negatively significant, as if decorated filaments drew in extra stain in this region. Sections shown are at the same axial position and have the same relative orientation. The average phase residual ( $\Psi \pm \text{SD}$ ), a measurement of the geometrical agreement among filaments generating reconstructions, was  $54.0 \pm 5.9^\circ$  for the F-actin-MLCK-147 data. The average up-down phase residual ( $\Delta\Psi \pm \text{SD}$ ), a measure of filament polarity, was  $23.7 \pm 8.5^\circ$ . The two values were comparable to those previously obtained.



eratively. The difference densities, attributable to the bound MLCK, were statistically significant at  $>99.95\%$  confidence levels. This analysis also showed that the protein-free pore between the MLCK density and F-actin (\* in b; cross-hatching in c) was negatively significant, as if decorated filaments drew in extra stain in this region. Sections shown are at the same axial position and have the same relative orientation. The average phase residual ( $\Psi \pm \text{SD}$ ), a measurement of the geometrical agreement among filaments generating reconstructions, was  $54.0 \pm 5.9^\circ$  for the F-actin-MLCK-147 data. The average up-down phase residual ( $\Delta\Psi \pm \text{SD}$ ), a measure of filament polarity, was  $23.7 \pm 8.5^\circ$ . The two values were comparable to those previously obtained.

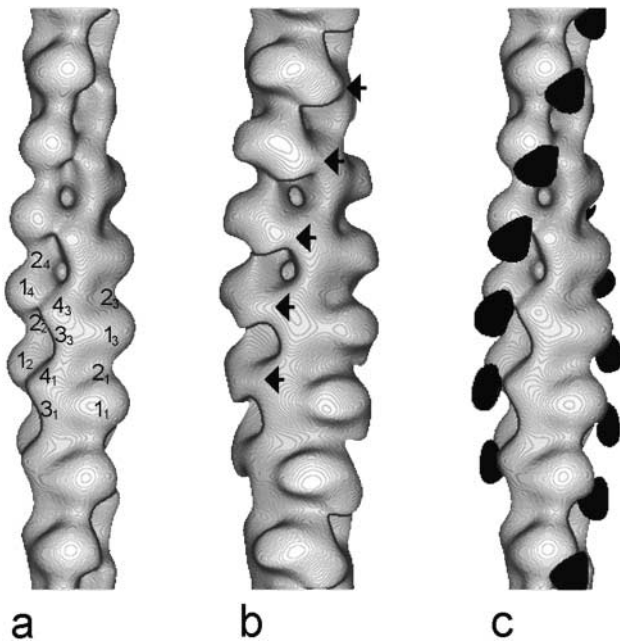


**Figure 3. Surface views of thin filament reconstructions showing the position of the MLCK-147 peptide on F-actin.** (a) F-actin control; actin subdomains are noted on four of the successive actin monomers (subscripts distinguish the particular monomer labeled; monomers with odd-numbered subscripts present face-on views of actin, and ones with even-numbered subscripts show reverse-side views). (b) MLCK-147-decorated F-actin; note the extra mass (arrows) not present in control filaments that link the bottom of subdomain-4 of each actin monomer to the back of subdomain-1 of the adjacent one. (c) To further define the relative position of MLCK-147, difference densities (filled black region) were calculated as described above and then superimposed on the F-actin reconstruction. Again, note the position of the difference density bridging between neighboring monomers and then extending downward toward the barbed end of the filament. Connectivity was not noted between axially adjacent MLCK-147 densities, and therefore the results did not allow us to determine if the MLCK peptide is arranged longitudinally along F-actin as suggested by binding studies (Smith and Stull, 2000). However, any possible linkage, predicted by Smith and Stull (2000), between successive binding domains may have been too thin or too disordered to be detected by the methods applied.

eratively, narrowing the  $\text{Ca}^{2+}$  concentration range required for regulation (Lehman et al., 2000). Smooth muscle and nonmuscle thin filaments also contain the protein caldesmon and smooth muscle filaments calponin, both often implicated in the regulation of thin filaments but of uncertain function despite extensive biochemical characterization (Marston and Huber, 1996; Chalovich et al., 1998; Marston et al., 1998; Winder et al., 1998). Structural information on the interactions of each of these proteins with F-actin has been extracted from three-dimensional (3-D) reconstructions (Vibert et al., 1993; Whittaker et al., 1995; Hodgkinson et al., 1997a,b; Lehman et al., 1997; Volkmann et al., 2000). Together, these proteins and myosin cover and/or move over much of the outer face of actin, leaving little room free for extra binding proteins, hence raising the possibility of a structural competition and functional clash with actin-bound MLCK. In the current report, the interactions of MLCK on F-actin were examined structurally. The site of MLCK binding was determined by electron microscopy and 3-D reconstruction to as-

sess if MLCK is specifically and uniquely localized on F-actin. We found that MLCK associates between laterally adjacent actin monomers on F-actin, over an unoccupied patch far from the myosin-binding site and from sites occupied by tropomyosin, caldesmon, and calponin on actin. Hence, MLCK binding should not interfere sterically with myosin cross-bridge cycling, cooperative activation by tropomyosin, or the operation of caldesmon or calponin.

## Results and discussion

### Electron microscopy of F-actin–MLCK-147 complexes

F-actin was complexed with peptide containing the  $\text{NH}_2$ -terminal 147 residues of MLCK (MLCK-147) under conditions that should saturate filaments with the protein. Electron micrographs of negatively stained filaments showed that the MLCK peptide caused extensive cross-linking of F-actin into loosely packed bundles and rafts. Only unbundled filaments within aggregates or those splaying off laterally were analyzed. Actin substructure, although evident, was frequently obscured by the binding of the MLCK-147 on the surface of filaments (Fig. 1), which also caused them to appear wider than pure F-actin. Globular structures were occasionally seen projecting from filaments but details of the shape, orientation, and periodicity of the MLCK peptide were not discernable. To detect the MLCK binding and determine its position on F-actin, image processing and 3-D reconstruction were therefore necessary.

### 3-D reconstructions of reconstituted thin filaments

Electron micrographs of two different sets of F-actin–MLCK-147 were analyzed independently by the first and last authors. Density maps of reconstituted filaments were calculated from the averages of the Fourier transform layer line data (not shown). All maps obtained showed typical two-domain actin monomers that could be further divided into identifiable subdomains (Figs. 2 and 3). When compared with maps generated from pure F-actin controls, each separately calculated reconstruction showed obvious extra density lying between the inner domain of one actin and the outer domain of the next monomer along the left-handed genetic helix of F-actin (Figs. 2 and 3, arrows). Since the two data sets were so similar, they were combined for further analysis. The extra mass, attributable to the MLCK peptide, and its location became especially apparent when difference densities computed between maps of F-actin–MLCK-147 and F-actin were superimposed on the F-actin reconstructions (filled black region in Figs. 2 and 3, respectively). The computed difference densities were statistically significant at confidence levels  $>99.95\%$ . The statistical analysis confirmed that the only significant difference between the control and MLCK maps was the mass bridging successive monomers. Inspection of the surface views of reconstructions (Fig. 3) showed that part of the MLCK density is connected to a relatively broad part of the back of actin subdomain-1. The opposite side of MLCK approaches a protuberance on the bottom of subdomain-4 of the next actin monomer along the F-actin genetic helix (subdomains noted on four successive actin monomers). The MLCK density therefore appears to link respective monomers together.



**Figure 4. Location of MLCK-147 densities on the atomic structure of F-actin.** The atomic model of F-actin (Lorenz et al., 1993) was fitted to the EM reconstructions as previously described (Vibert et al., 1997), and the location of the MLCK difference density on the atomic model was established. Two neighboring actin monomers are displayed as  $\alpha$ -carbon chains: one in green (face-on view of actin) and the other in yellow (reverse-side view; note that these two monomers correspond to actin monomers 1 and 2 in Fig. 3). The fitted MLCK density (red) approaches an  $\alpha$ -helix projecting from actin subdomain-4 on one monomer (residues 228–232 highlighted in magenta) and comes into close contact with the COOH-terminal  $\alpha$ -helix of actin subdomain-1 on the other (residues 364–375 highlighted in white). Without an atomic model of MLCK-147 available as a reference for molecular fitting, an exact description of the volume, shape, orientation, and contact points of the MLCK density on F-actin is precluded by the resolution and positional accuracy of the data.

#### Fitting MLCK on the atomic model of F-actin

To further define the MLCK-147 binding site on F-actin, the MLCK difference densities were localized on the refined atomic model of F-actin (Lorenz et al., 1993) by fitting the atomic model within the envelope formed by the actin component of our reconstructions (compare with Vibert et al., 1997). The fitting (Fig. 4) indicated that one side of MLCK-147 (red) attached to COOH-terminal residues on subdomain-1 of one actin monomer and that the opposite side of the peptide closely approached an  $\alpha$ -helix (representing actin residues 228–232) protruding from subdomain-4 of the neighboring monomer. The MLCK binding site is distinct from consensus actin binding sites previously observed (McGough, 1998).

#### Molecular model of MLCK–actin binding

Circular dichroism studies indicate that MLCK-147 is largely unstructured without  $\alpha$ -helix and  $\beta$ -sheet content (unpublished data). Despite this, our observations here indicate that, once associated with F-actin, MLCK-147 assumed a fairly compact shape, as if a structured conformation was induced by binding to actin. Further inspection of the resi-

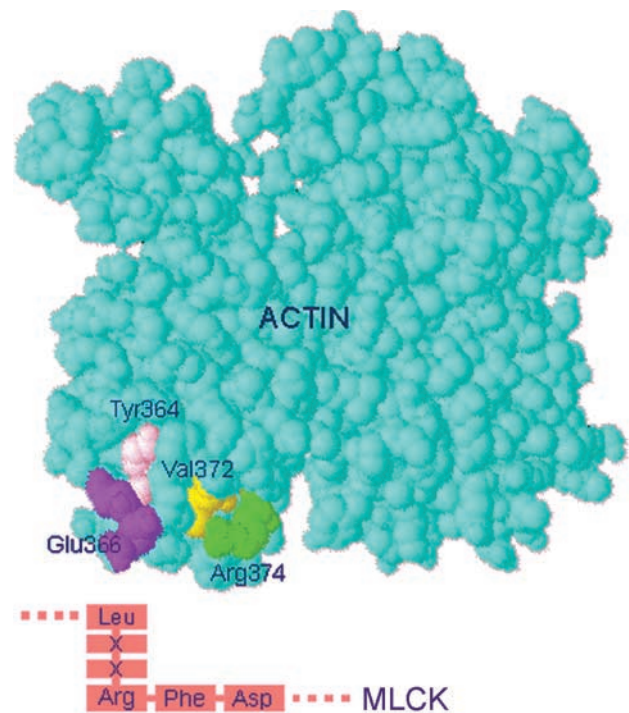


**Figure 5. Space-filling model of actin showing possible sites of interaction with the MLCK-binding motif.** The amino acid sequence and 3-D structure of chicken aortic actin were evaluated in light of both the molecular fitting depicted in Fig. 4 and data on the DFRXXL binding motif. The space-filling model shows that the COOH-terminal actin residues Arg374 (green), Val372 (yellow), Glu366 (magenta), and Tyr364 (off-white) on the actin surface could make alternating electrostatic and hydrophobic interactions with DFRXXL (drawn schematically). If this were true, then the apparent binding to residues 228–232 of a laterally adjacent actin monomer (as in Fig. 4) would occur with flanking amino acids of the MLCK-147 construct.

dues involved in the docking site of MLCK on actin revealed a stretch of charged and hydrophobic residues at the COOH-terminal region of F-actin complementary to those in the MLCK-147 binding motif, suggesting that binding might occur as illustrated in the model in Fig. 5, in which the DFRXXL residues of MLCK-147 associate with the Arg374, Val372, Glu366, and Tyr364 of actin, respectively.

#### Comparison of binding of MLCK and other actin-binding proteins

The amount of MLCK in smooth muscle and nonmuscle cells is substantially less than the amount of actin-binding sites (Hartshorne, 1987; Stull et al., 1998), and it is therefore likely that MLCK will be targeted to actin filaments participating in myosin II–based motility (compare with North et al., 1994a; Kamm and Stull, 2001). These filaments contain several actin-binding proteins involved in regulating thin filament function that could potentially compete with MLCK for actin-binding sites. Since the locations of all major smooth muscle and key nonmuscle thin filament-associated proteins are known, their binding and that of MLCK could be compared structurally. Inspection of Fig. 6, a composite of difference density maps localizing the myosin binding site and positions of tropomyosin, caldesmon, calponin, and

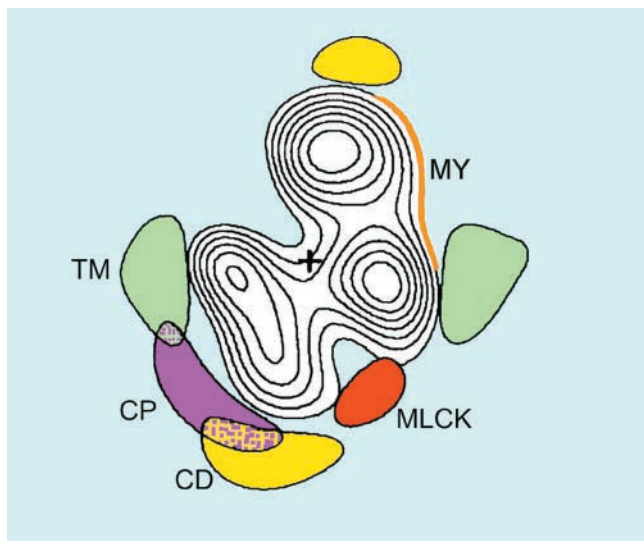


**Figure 6. Composite map displaying the relative positions of smooth muscle actin-binding proteins.** Binding locations of MLCK-147 (red), smooth muscle tropomyosin (TM, green; data from Lehman et al., 2000), calponin (CP, magenta; data from Hodgkinson et al., 1997a), and caldesmon (CD, yellow; derived from selected data in Hodgkinson et al., 1997b) were plotted on a transverse section of F-actin. The myosin-binding site on actin (from data of S-1-decorated thin filaments in Milligan et al., 1990; Vibert et al., 1997) is highlighted (MY, ochre). Note that the MLCK-binding site is far from each of the other actin-binding proteins.

MLCK-147 on F-actin, demonstrates that the MLCK docking site is distinct from that of the others. The absence of any steric clash between the binding of MLCK and the other actin-binding proteins would favor the stability of the MLCK interaction. Moreover, the unique binding of MLCK would not interfere with myosin docking and cycling on actin. It is noteworthy that caldesmon and calponin densities do overlap structurally with each other (Fig. 6), consistent with significant binding competition of caldesmon and calponin observed *in vitro* and histological segregation *in vivo* (Fürst et al., 1986; Small et al., 1986; Lehman, 1991; Makuch et al., 1991; North et al., 1994a,b); in contrast, MLCK binding to native smooth muscle thin filaments is not blocked by the presence of tropomyosin, caldesmon, and/or calponin (Smith et al., 1999). Together, studies on the structure of smooth muscle thin filaments demonstrate that actin-binding proteins adopt characteristic positions on the thin filament consistent with distinct functions. In the case of the short MLCK in smooth muscle, its NH<sub>2</sub>-terminal structural domain is anchored to a site where no other actin-binding protein to date has been localized (compare with McGough, 1998). The long MLCK present in nonmuscle cells has two additional DFRXXL actin-binding motifs, and thus, it is predicted that its location will be similar except for a maximal stoichiometry of one long MLCK per five actin monomers in the thin filament. In both the short and long MLCKs, the intervening PEVK, Ig-like, and fibronectin modules would extend the catalytic core to myosin thick filaments, thereby allowing regulatory light chain phosphorylation upon activation by Ca<sup>2+</sup>-calmodulin. The design of the MLCK molecule is therefore well adapted for its part in the cascade of events leading to myosin II-based cellular motility.

## Materials and methods

### Protein preparation

Construction and expression of MLCK-147: the cDNA fragment of the NH<sub>2</sub>-terminal 1–147 amino acids of rabbit smooth muscle MLCK was amplified by PCR and subcloned into TOPO cloning vector pCR 2.1 (Invitrogen). After sequencing, the cDNA was then subcloned into the expression vector pET 28a (Novagen) with a His-tag sequence at the NH<sub>2</sub> terminus of MLCK-147. The expression constructs were transformed into bacteria strain BL21 (DE3), and protein expression was induced by IPTG. After centrifugation, the cells were resuspended in 20 mM Tris/HCl, pH 7.0, 1 mM EDTA, and 0.1% NP-40, sonicated, and centrifuged again. The soluble MLCK-147 peptide was purified by His-Bind Quick column as described by the manufacturer (Novagen). The purified MLCK-147 binds to F-actin with a *K<sub>d</sub>* value of  $0.26 \pm 0.01 \mu\text{M}$  and a stoichiometry of one MLCK-147 to three actin molecules. MLCK-147 contains the three DFRXXL motifs present in the 75-amino acid NH<sub>2</sub>-terminal fragment studied by Smith and Stull (2000).

Rabbit skeletal muscle F-actin was purified by standard methods (Spudich and Watt, 1971). The F-actin used was stable and did not aggregate, an advantage for the structural studies performed. Different actin isoforms are highly conserved (we used skeletal muscle  $\alpha$ -actin in our studies); isoform variability, in fact, occurs mainly at the acidic NH<sub>2</sub>-terminal six amino acids of actin (Vanderkerckhove and Weber, 1978; Lehman et al., 1996) whose position is distal from the site of MLCK-147 binding (see Results and discussion). There were no significant differences in binding affinity of NH<sub>2</sub>-terminal MLCK fragments to skeletal muscle F-actin and detergent washed native smooth muscle myofilaments; the stoichiometry of binding was the same (Smith and Stull, 2000; unpublished data).

### Electron microscopy and helical reconstruction

F-actin (1  $\mu\text{M}$ ) was decorated with excess MLCK-147 (2  $\mu\text{M}$ ) in solutions of 50 mM KCl, 1 mM EGTA, 1 mM MgCl<sub>2</sub>, 0.2 mM ATP, 1 mM DTT, 10 mM imidazole buffer (pH 7.2) at room temperature ( $\sim 25^\circ\text{C}$ ). Reconstituted filaments were immediately applied to carbon-coated electron microscope grids and negatively stained as previously described (Moody et al., 1990). Prolonged decoration was avoided, since F-actin and MLCK-147 incubated together for as short as 5 min formed very large and unusable filament aggregates. Electron micrograph images of decorated filaments were recorded on a Philips CM120 electron microscope at 60,000 $\times$  magnification under low-dose conditions ( $\sim 12\text{e}^-/\text{\AA}^2$ ). Micrographs were digitized using a ZEISS SCAI scanner at a pixel size corresponding to 0.7 nm in the filaments. Well-stained regions of filaments were selected and straightened as previously described (Egelman, 1986; Hodgkinson et al., 1997a). Helical reconstruction was carried out by standard methods (DeRosier and Moore, 1970; Amos and Klug, 1975; Owen et al., 1996) as previously described (Vibert et al., 1993, 1997). Two independently analyzed sets of filaments totaling 28 filaments were chosen for averaging, based on their relative phase agreement. The reconstruction had a resolution (Owen and DeRosier, 1993) of 2.5–3.0 nm; the positional accuracy of the method is  $\sim 0.5$  nm (Milligan et al., 1990). Difference density analysis to define MLCK position on actin was carried out as previously described (Xu et al., 1999), and differences between maps were evaluated statistically using a Student's *t* test (Milligan and Flicker, 1987; Trachtenberg and DeRosier, 1987). Fitting of reconstructions to the atomic resolution structure of F-actin (Lorenz et al., 1993) was carried out as previously described (McGough and Way, 1995; Vibert et al., 1997; Xu et al., 1999) using the program O (Jones et al., 1991).

This work was supported by National Institutes of Health grants HL-36153 (to W. Lehman), HL-26043 (to J.T. Stull), and HL-62468 (to R. Craig) and by Shared Instrumentation grant RR-08426 (to R. Craig).

Submitted: 15 May 2001

Revised: 13 June 2001

Accepted: 3 July 2001

## References

- Amos, L.A., and A. Klug. 1975. Three-dimensional image reconstruction of the contractile tail of T4 bacteriophage. *J. Mol. Biol.* 99:51–73.
- Chalovich, J.M., A. Sen, A. Resetar, B. Leinweber, R.S. Fredricksen, F. Lu, and Y.-D. Chen. 1998. Caldesmon: binding to actin and myosin and effects on the elementary steps in the ATPase cycle. *Acta Physiol. Scand.* 164:427–435.
- Cohen, P. 2000. The regulation of multisite phosphorylation—a 25 year update. *Trends Biochem. Sci.* 25:596–601.
- Dabrowska, R., S. Hinkins, M.P. Walsh, and D.J. Hartshorne. 1982. The binding

- of smooth muscle myosin light chain kinase to actin. *Biochem. Biophys. Res. Commun.* 107:1524–1531.
- DeRosier, D.J., and P.B. Moore. 1970. Reconstruction of three-dimensional images from electron micrographs of structures with helical symmetry. *J. Mol. Biol.* 52:355–369.
- Egelman, E.H. 1986. An algorithm for straightening images of curved filamentous structures. *Ultramicroscopy.* 19:367–374.
- Erdödi, F., M. Ito, and D.J. Hartshorne. 1996. Myosin light chain phosphatase. In *Biochemistry of Smooth Muscle Contraction*, M. Bárány, editor. Academic Press, San Diego. 131–141.
- Fürst, D.O., R.A. Cross, J. DeMey, and J.V. Small. 1986. Caldesmon is an elongated flexible molecule localized in the actomyosin domains of smooth muscle. *EMBO J.* 5:251–257.
- Gallagher, P.J., and J.T. Stull. 1997. Localization of an actin binding domain in smooth muscle myosin light chain kinase. *Mol. Cell. Biochem.* 173:1–57.
- Guerriero, V., D.R. Rowley, and A.R. Means. 1981. Production and characterization of an antibody to myosin light chain kinase and intracellular localization of the enzyme. *Cell.* 27:449–458.
- Hartshorne, D.J. 1987. Biochemistry of the contractile process in smooth muscle. In *Physiology of the Gastrointestinal Tract*, L.R. Johnson, editor. Raven Press, New York. 423–482.
- Herring, B.P., S. Dixon, and P.J. Gallagher. 2000. Smooth muscle myosin light chain kinase expression in cardiac and skeletal muscle. *Am. J. Physiol.* 279: C1656–C1664.
- Hodgkinson, J.L., M. EL-Mezgueldi, R. Craig, P. Vibert, S.B. Marston, and W. Lehman. 1997a. 3-D image reconstruction of reconstituted smooth muscle thin filaments containing calponin: visualization of interactions between F-actin and calponin. *J. Mol. Biol.* 273:150–159.
- Hodgkinson, J.L., S.B. Marston, R. Craig, P. Vibert, and W. Lehman. 1997b. Three-dimensional image reconstruction of reconstituted smooth muscle thin filaments: effects of caldesmon. *Biophys. J.* 72:2398–2404.
- Jones, T.A., J.Y. Zou, S.W. Cowan, and M. Kjeldgaard. 1991. Improved methods for the building of protein models in electron density maps and the location of errors in these models. *Acta Crystallogr.* 47:110–119.
- Kamm, K., and J.T. Stull. 1985. The function of myosin and myosin light chain kinase phosphorylation in smooth muscle. *Annu. Rev. Pharmacol. Toxicol.* 25:593–620.
- Kamm, K.E., and J.T. Stull. 2001. Dedicated myosin light chain kinases with diverse cellular functions. *J. Biol. Chem.* 276:4527–4530.
- Kanoh, S., M. Ito, E. Niwa, Y. Kawano, and D.J. Hartshorne. 1993. Actin-binding peptide from smooth muscle myosin light chain kinase. *Biochemistry.* 32: 8902–8907.
- Lehman, W. 1991. Calponin and the composition of smooth muscle thin filaments. *J. Muscle Res. Cell Motility.* 12:221–224.
- Lehman, W., P. Vibert, R. Craig, and M. Bárány. 1996. Actin and the structure of thin filaments. In *Biochemistry of Smooth Muscle Contraction*. M. Bárány, editor. Academic Press, San Diego. 47–62.
- Lehman, W., P. Vibert, and R. Craig. 1997. Visualization of caldesmon on smooth muscle thin filaments. *J. Mol. Biol.* 274:310–317.
- Lehman, W., V. Hatch, V. Korman, M. Rosol, L. Thomas, R. Maytum, M.A. Geeves, J.E. Van Eyk, L.S. Tobacman, and R. Craig. 2000. Tropomyosin isoforms modulate the localization of tropomyosin strands on actin filaments. *J. Mol. Biol.* 302:593–606.
- Lin, P.-J., K. Luby-Phelps, and J.T. Stull. 1997. Binding of myosin light chain kinase to cellular actin-myosin filaments. *J. Biol. Chem.* 272:7412–7420.
- Lin, P.-J., K. Luby-Phelps, and J.T. Stull. 1999. Properties of filament-bound myosin light chain kinase. *J. Biol. Chem.* 274:5987–5994.
- Lorenz, M., D. Popp, and K.C. Holmes. 1993. Refinement of the F-actin model against x-ray fiber diffraction data by use of a directed mutation algorithm. *J. Mol. Biol.* 234:826–836.
- MacDonald, J.A., M.A. Borman, A. Muranyi, A.V. Somlyo, D.J. Hartshorne, and T.A. Haystead. 2001. Identification of the endogenous smooth muscle phosphatase-associated kinase. *Proc. Natl. Acad. Sci. USA.* 98:2419–2424.
- Makuch, R., K. Birukov, V. Shirinsky, and D. Dabrowska. 1991. Functional interrelationship between calponin and caldesmon. *Biochem. J.* 280:33–38.
- Marston, S.B., and P.A.J. Huber. 1996. Caldesmon. In *Biochemistry of Smooth Muscle Contraction*. M. Bárány, editor. Academic Press, San Diego, CA. 119–130.
- Marston, S.B., D. Burton, O. Copeland, I. Fraser, Y. Gao, J. Hodgkinson, P. Huber, B. Levine, M. EL-Mezgueldi, and G. Notarianni. 1998. Structural interactions between actin, tropomyosin, caldesmon and calcium binding protein and the regulation of smooth muscle thin filaments. *Acta Physiol. Scand.* 164:401–414.
- McGough, A. 1998. F-actin-binding proteins. *Current Opin. Struct. Biol.* 8:166–176.
- McGough, A., and M. Way. 1995. Molecular model of an actin filament capped by a severing protein. *J. Struct. Biol.* 115:144–150.
- Milligan, R.A., and P.F. Flicker. 1987. Structural relationships of actin, myosin, and tropomyosin revealed by cryo-electron microscopy. *J. Cell Biol.* 105:29–39.
- Milligan, R.A., M. Whittaker, and D. Safer. 1990. Molecular structure of F-actin and the location of surface binding sites. *Nature.* 348:217–221.
- Moody, C., W. Lehman, and R. Craig. 1990. Caldesmon and the structure of vertebrate smooth muscle thin filaments: electron microscopy of isolated thin filaments. *J. Muscle Res. Cell Motility.* 11:176–185.
- North, A.J., M. Gimona, Z. Lando, and J.V. Small. 1994a. Actin isoform compartments in chicken gizzard smooth muscle cells. *J. Cell Sci.* 107:445–455.
- North, A.J., M. Gimona, R.A. Cross, Z. Lando, and J.V. Small. 1994b. Calponin is localised in both the contractile apparatus and the cytoskeleton of smooth muscle cells. *J. Cell Sci.* 107:437–444.
- Nunnally, M., and J.T. Stull. 1984. Mammalian skeletal muscle myosin light chain kinases: a comparison by antiserum cross-reactivity. *J. Biol. Chem.* 259: 1776–1780.
- Owen, C., and D.J. DeRosier. 1993. A 13-Å map of the actin–troponin filament from the *Limulus* acrosomal process. *J. Cell Biol.* 123:337–344.
- Owen, C., D.G. Morgan, and D.J. DeRosier. 1996. Image analysis of helical objects: the Brandeis helical package. *J. Struct. Biol.* 116:167–175.
- Perry, S.V. 1983. Phosphorylation of the myofibrillar proteins and the regulation of contractile activity in muscle. *Philos. Trans. Roy. Soc. B.* 302:59–71.
- Sellers, J.R., and R.S. Adelstein. 1986. Regulation of contractile activity. In *The Enzymes*. P.D. Boyer and E.G. Krebs, editors. Academic Press, Orlando, FL. 381–418.
- Sellers, J.R., and M.D. Pato. 1984. The binding of smooth muscle myosin light chain kinase and phosphatases to actin and myosin. *J. Biol. Chem.* 259:740–746.
- Small, J.V., D.O. Fürst, and J. DeMey. 1986. Localization of filamin in smooth muscle. *J. Cell Biol.* 102:210–220.
- Smith, L., and J.T. Stull. 2000. Myosin light chain kinase binding to actin filaments. *FEBS Lett.* 480:298–300.
- Smith, L., X. Su, P.-J. Lin, and J.T. Stull. 1999. Identification of a novel actin binding motif in smooth muscle light chain kinase. *J. Biol. Chem.* 274: 29433–29438.
- Somlyo, A.P., and A.V. Somlyo. 2000. Signal transduction by G-proteins, rho-kinase and protein phosphatase to smooth muscle and non-muscle myosin II. *J. Physiol.* 522:177–185.
- Spudich, J.A., and S. Watt. 1971. The regulation of rabbit skeletal muscle contraction. I. Biochemical studies of the interaction of the tropomyosin-troponin complex with actin and the proteolytic fragments of myosin. *J. Biol. Chem.* 242:4866–4871.
- Stull, J.T., J.K. Krueger, K.E. Kamm, Z.-H. Gao, G. Zhi, and R. Padre. 1996. Myosin light chain kinase. In *Biochemistry of Smooth Muscle Contraction*. M. Bárány, editor. Academic Press, San Diego. 119–130.
- Stull, J.T., K.E. Kamm, J.K. Krueger, P. Lin, K. Luby-Phelps, and G. Zhi. 1997. Ca<sup>2+</sup>/calmodulin-dependent myosin light-chain kinases. *Adv. Second. Messenger. Phosphoprotein Res.* 31:141–150.
- Stull, J.T., P.-J. Lin, J.K. Krueger, J. Trehwella, and G. Zhi. 1998. Myosin light chain kinase: functional domains and structural motifs. *Acta Physiol. Scand.* 164:471–482.
- Tansey, M.G., K. Luby-Phelps, K.E. Kamm, and J.T. Stull. 1994. Ca<sup>2+</sup>-dependent phosphorylation of myosin light chain kinase decreases the Ca<sup>2+</sup> sensitivity of light chain phosphorylation within smooth muscle cells. *J. Biol. Chem.* 269:9912–9920.
- Trachtenberg, S., and D.J. DeRosier. 1987. Three-dimensional structure of the frozen-hydrated flagellar filament: the left-handed filament of *Salmonella typhimurium*. *J. Mol. Biol.* 195:581–601.
- Vanderkerckhove, J., and K. Weber. 1978. At least 6 different actins are expressed in a higher mammal. *J. Mol. Biol.* 126:783–802.
- Vibert, P., R. Craig, and W. Lehman. 1993. Three-dimensional reconstruction of caldesmon-containing smooth muscle thin filaments. *J. Cell Biol.* 123:313–321.
- Vibert, P., R. Craig, and W. Lehman. 1997. Steric-model for activation of muscle thin filaments. *J. Mol. Biol.* 266:8–14.
- Volkman, N., D. Hanein, G. Ouyang, K.M. Trybus, D.J. DeRosier, and S. Lowey. 2000. Evidence for cleft closure in actomyosin upon ADP release. *Nat. Struct. Biol.* 7:1147–1155.
- Whittaker, M., E.M. Wilson-Kubalek, J.E. Smith, L. Faust, R.A. Milligan, and

- H.L. Sweeney. 1995. A 35-movement of smooth muscle myosin on ADP release. *Nature*. 378:748–751.
- Winder, S.J., B.G. Allen, O. Clement-Chomienne, and M.P. Walsh. 1998. Regulation of smooth muscle actin-myosin interaction and force by calponin. *Acta Physiol. Scand.* 164:415–426.
- Xu, C., R. Craig, L. Tobacman, R. Horowitz, and W. Lehman. 1999. Tropomyosin positions in regulated thin filaments revealed by cryoelectron microscopy. *Biophys. J.* 77:985–992.
- Ye, L.-H., K. Hayakawa, H. Kishi, M. Imamura, A. Nakamura, T. Okagaki, T. Takagi, A. Iwata, T. Tanaka, and K. Kohama. 1997. The structure and function of the actin-binding domain of myosin light chain kinase of smooth muscle. *J. Biol. Chem.* 272:32182–32189.